How bead size and dielectric constant affect the plasma behaviour in a packed bed plasma reactor : a modelling study

How bead size and dielectric constant affect the plasma behaviour in a packed bed plasma reactor: a modelling study

Koen Van Laer*, Annemie Bogaerts

K. Van Laer, Prof. Dr. A. Bogaerts,

Research group PLASMANT, Department of Chemistry, University of Antwerp, Universiteitsplein 1, 2610 Wilrijk-Antwerp, Belgium

E-mail: koen.vanlaer@uantwerpen.be

Abstract

Packed bed plasma reactors (PBPRs) are gaining increasing interest in recent years for use in environmental applications, such as greenhouse gas conversion into value-added chemicals or renewable fuels and volatile pollutant removal (e.g. NOx, VOC, …), as they enhance the conversion and energy efficiency of the process compared to a non-packed reactor. However, the

plasma behaviour in a PBPR is not well understood. In this paper we demonstrate, by means of a fluid model, that the discharge behaviour changes considerably when changing the size of the packing beads and their dielectric constant, while keeping the interelectrode spacing constant. At low dielectric constant, the plasma is spread out over the full discharge gap, showing significant density in the voids as well as in the connecting void channels. The electric current profile shows a strong peak during each half cycle. When the dielectric constant increases, the plasma becomes localised in the voids, with a current profile consisting of many smaller peaks during each half cycle. For large bead sizes, the shift from full gap discharge to localised discharges takes place at a higher dielectric constant than for smaller beads. Furthermore, smaller beads or beads with a lower dielectric constant require a higher breakdown voltage to cause plasma formation.

1. Introduction

Packed bed dielectric barrier discharge (DBD) reactors are receiving more and more attention for environmental applications, such as greenhouse gas conversion and volatile pollutant removal (e.g. NOx, VOC, …).[1-11] The packing beads lead to an enhanced electric field near the contact points, resulting in higher electron energies, causing more electron impact collisions and thus a greater production of reactive species, than in an empty DBD reactor. If the packing beads are catalytically active or coated with a catalytic material, they can even steer the process towards a preferred end product, in so-called plasma catalysis.[12-13] However, the factors leading to the experimentally observed synergy between plasma and catalysis are still very much under investigation.

The improved performance of a PBPR is observed in many experimental studies.[1-11] However, the exact behaviour of the plasma, such as its ignition and propagation through the packing material, is not so well described. The plasma formation and propagation is much more defined by local effects, for instance the electric field enhancement near the contact points, which is difficult to separate from the global experimental results. Furthermore, the presence of the packing beads also blocks the visual path for optical diagnostics. A computational study can therefore be very interesting, to achieve a better understanding of the discharge behaviour in a PBPR.

The number of computational studies on a PBPR is, however, limited. Chang and Takaki et al. developed a simplified time-averaged 1D numerical plasma model for N_2, based on solving Poisson's equation and transport equations.[14-15] They found that all plasma parameters increase upon increasing applied potential and dielectric constant. Due to the 1D limitation, the

void between the beads was simply assumed to be spherical. Kang et al. studied the first 20 ns of the propagation of the microdischarges formed in a 2D model of a DBD reactor with two stacked ferroelectric beads inside.[16] Russ et al. used a 2D fluid model to simulate the formation of microdischarges in a packed bed DBD reactor filled with dry exhaust gas (N_2/O_2 = 80/20 and 500 ppm NO).[17] The work was limited to a short one-directional discharge with a constant applied potential. Although not directly applied to a packed bed reactor, Babaeva et al. performed very relevant modelling work on the influence of dielectric spheres blocking a plasma streamer, using a 2D fluid model in humid air ($N_2/O_2/H_2O$ = 79.5/19.5/1).[18] More recently, Kruszelnicki et al. studied the propagation of negative electrical discharges in a PBPR with a combination of a 2D fluid model and a purpose-built experimental setup.[19] Surface ionization waves (SIWs) and positive restrikes were shown to be mainly responsible for reactive species production. Finally, Zhang et al. applied a 2D particle-in-cell / Monte Carlo collision (PIC/MCC) model to describe the filamentary discharge behaviour in a packed bed DBD reactor in air (N_2/O_2 = 80/20).[20]

In our previous work, we presented two complementary 2D axisymmetric fluid models for a PBPR in helium, and we studied the influence of the applied potential [21]. Furthermore, we also compared a millimetre-scale and microscale reactor, for a wide range of dielectric constants of the packing beads, to study the initiation and propagation of a helium plasma.[22] We found that the discharge always initiates at the position of the highest electric field and electron temperature, which is near the contact points. At sufficiently high applied potential, the discharge was able to spread across the gas gap, travelling through the “channels” in between the packing beads. Reducing the size of the reactor and/or increasing the dielectric constant of the packing

strongly influenced the discharge behaviour, shifting from fewer strong discharges over the total discharge gap to a larger number of smaller and more localised discharges.

In this paper, we investigate the influence of the size of the packing beads and their dielectric constant on the discharge behaviour, with the interelectrode spacing kept constant. Indeed, experiments have demonstrated that changing the packing size can drastically affect the performance of the application.[23-26]

Butterworth et al. studied CO_2 splitting in a PBPR with five different bead sizes for two different bead materials, namely Al_2O_3 and $BaTiO_3$, changing the gas composition from 90/10 Ar/CO_2 to pure CO_2.[23] They concluded that smaller packing beads can significantly increase the CO_2 conversion, given that the applied potential is sufficiently high to cause a discharge in the void spaces, because a smaller packing also leads to a higher breakdown voltage. However, this only applies when argon is used as carrier gas. With pure CO_2 the benefits of smaller packing beads are mitigated, and even reversed. Michielsen et al. confirmed that for pure CO_2 the largest beads perform the best.[24] However, the results strongly depend on the bead material, with the highest conversions and energy efficiencies being found with $BaTiO_3$.

In our own previous experimental study we found that also the input power can be of great importance.[10] The best combination of both CO_2 conversion and energy efficiency, in case of zirconia beads, was found using the lowest input power and the largest beads. However, at higher input power, smaller bead sizes gave the best combined results. Lastly, Duan et al. studied the splitting of CO_2 in a packed bed microreactor.[25] They gained the best results using the smallest packing beads with the highest dielectric constant, which in their study was CaO ($\varepsilon \sim 12$). However, the CO_2 capturing abilities of CaO, which were not mentioned in the paper, probably

contributed to the higher reported conversions, without actually being attributed to CO_2 splitting into CO and O_2.

From these experimental studies, it is clear that there is no simple rule regarding the bead size that ensures the best results. As far as the dielectric constant of the beads is concerned, however, the higher values seem to lead to higher conversion and efficiency rates in all these studies. Nevertheless, it is made clear in literature that also other material parameters, such as the porosity, surface morphology, acid-base properties, etc. play a role.[8, 24, 27] For example, Yu et al. observed a higher CO_2 conversion when using a quartz packing with sharp edges instead of a smooth silica bead packing, even though they have the same dielectric constant.[8] The sharp edges increase the electric field enhancement at the contact points, leading to a higher overall conversion, as reported in literature.[15, 26] Furthermore, the higher conversion reached with γ-Al_0O_3 versus α-Al_2O_3 was explained by the superior chemisorption abilities of γ-Al_2O_3 which promote the adsorption of CO_2 versus the chemically inert α-Al_2O_3 which lacks this ability.[8]

Veerapandian et al. wrote an interesting review on the influence of the different material properties on the VOC removal efficiency, based on experimental as well as modelling research.[27] It is revealed that a higher dielectric constant leads to a higher decomposition efficiency. However, its influence saturates at a particular dielectric constant. The size of the packing is important to maximize the number of contact points without overly reducing the open spaces in the reactor, since these are needed to facilitate the generation of plasma. The shape of the packing can influence the electric field enhancement when sharp edges are present (as mentioned before). Porous material will enhance the residence time and surface area for possible chemisorption. Furthermore, depending on the bead size, additional microdischarges can be formed inside the pores, enhancing the discharge power. However, coking in the pores over time

is a serious problem. Depending on the material, the selectivity towards unwanted by-products can also be altered. It is clear that the modification of the packing beads towards the best possible results is an important but complicated exercise to be made, in order to improve the application of interest.

To aid in the understanding process, modelling is an interesting tool to help explain the present and future experimental results. We believe that the ability to focus on the change of one material property at a time is one of the greatest advantages of modelling.

In a broader perspective, our study can also be relevant for any atmospheric plasma research where objects are blocking the path of the plasma propagation, such as plasma jets interfering with any medium, from a dust particle to tissue.[28-31]

2. Model description

The fluid model is developed with COMSOL Multiphysics' built-in plasma module (version 5.0).[32] The model is based on solving a set of coupled differential equations that express the conservation of mass, momentum and energy, for the different plasma species (see below). In addition, the Poisson equation self-consistently calculates the electric field distribution based on the calculated charged species densities at each time step. For a more detailed explanation about the equations solved, we refer to our previous paper.[21]

The used geometries in the model are based on a 3D unit cell, as it would appear in a real life packed bed reactor. For the ease of calculation the surfaces of the dielectric and grounded electrode are flat, representing a reactor in planar configuration, but the results can equally be applied to a cylindrical reactor, as the curvature over the size of one unit cell would not be large. Due to calculation time issues we are not able to solve our model in 3D, because this would at least require several months for a single calculation. Therefore, we need to use smart approximations, resulting in a 2D axisymmetric geometry. The reasoning behind these approximations can be found in our previous publications.[21, 22] We realize that the 2D approximation would lead to a torus for the pellets on the right, in a 3D geometry, but we are interested in the plasma behaviour in between the packing beads, and we believe that the latter will not be affected by this torus shape.

We study the packed bed DBD reactor, with 3, 5 and 9 packing beads, as shown in figure 1, with diameter of 2.00 mm, 1.20 mm and 0.75 mm, respectively, keeping the discharge gap size fixed at 4.50 mm. Only the powered electrode, at the top, is covered with dielectric material ($\varepsilon = 9$, equivalent to alumina). The bottom electrode is grounded. The different packing beads in

the reactor are not touching each other, to account for the void space which is present in the real 3D geometry, while using a 2D model for the sake of computation time. The closest distance between the packing beads is related to their diameter. More specifically, it is equal to the diameter of the sphere enclosed by three touching beads in the same plane, representing the smallest possible opening between the beads in a real 3D close-packed reactor.

Although the PBPR configuration is mostly used for environmental applications, and thus with molecular gases, we apply the model in this study to helium, for two reasons. First of all, the reaction set of this noble gas is quite simple, therefore limiting the calculation time. Secondly, it has the ability to form a homogeneous discharge, which fits the used fluid description. We are aware that molecular gases, such as CO_2, typically show a filamentary discharge in a DBD reactor. However, when a packing is introduced, the filamentary discharge behaviour is affected, showing more localised discharges consisting of local streamers and surface discharges. The correct calculation of this behaviour requires the inclusion of photoionization, which will further increase the calculation time significantly. There exist some modelling papers in literature where photoionization is included to describe this behaviour [18,19], but in these cases the calculated time was kept very small, in the order of tens of nanoseconds, which is far from the time-scale of a few periods of applied potential as we simulate in our study. These calculation time issues are the main reason why we use helium when studying a PBPR. We are aware that a direct comparison of our modelling results with experimental data for environmental applications is not possible. However, we will try to extrapolate, with the necessary carefulness, our modelling results onto the experimental observations in order to help explain and understand them.

In the helium chemistry set, we consider 6 species, i.e. electrons, neutral helium atoms, positive atomic and molecular ions, two metastable helium atoms (2^1S and 2^3S) lumped into one effective level, and helium dimers. These species react with each other in 23 different reactions. The complete reaction set and the transport coefficients used for these species can be found in our previous paper.[21]

The dielectric material and the exposed electrode are treated as smooth objects without any surface roughness or pores. The dielectric material is treated with conservation of charge inside the material and charge accumulation on its surface. The outer boundary on the right in figure 1 is treated with an insulation boundary condition, forcing the normal fluxes of electrons and electron energy to zero, and a zero charge boundary condition, which states the normal electric displacement field to be zero as well. This combination of boundary conditions implies periodicity on the outer boundary with a zero gradient of charged species across it. The boundary on the left is the symmetry axis, typically treated with a no-flux boundary condition.

At the walls, i.e., the packing beads, the top dielectric and the bottom electrode, we assume quenching of atomic and molecular metastables, and electron-ion recombination of atomic and molecular ions. These last two processes have a probability of 0.05 to emit a secondary electron with energy of 5 eV.[33] This parameter is kept constant regardless of the bead material. The pressure and temperature are fixed at 1 atm and 300 K, respectively. The dielectric constant of the packing beads is varied, and the values match different possible packing materials, namely 5 (glass), 9 (alumina), 25 (zirconia), 100 (titania) and 1000 (ferroelectric materials, like $BaTiO_3$). Note, however, that the named materials are just for indication purposes, since their other properties, for example the porosity, are not yet taken into account in this study.

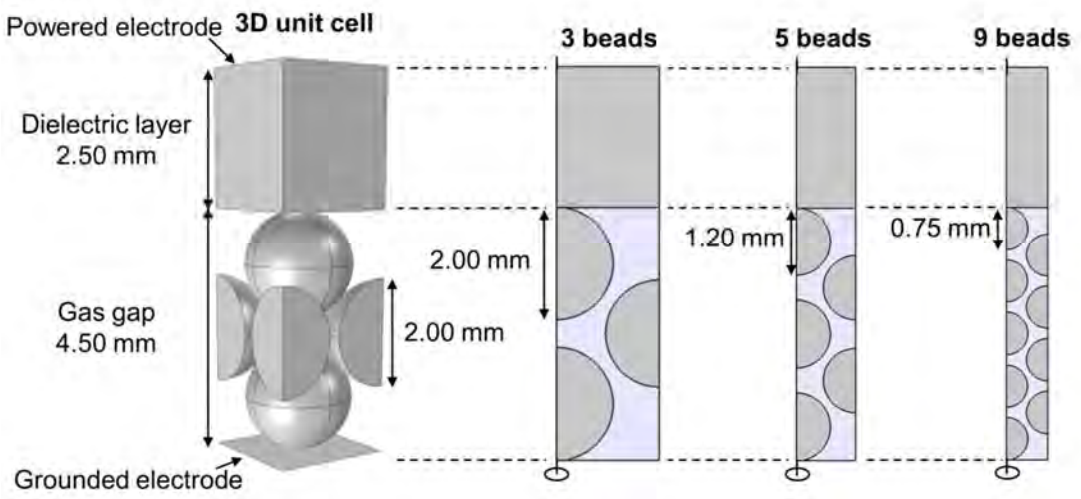

Figure 1: 3D unit cell of a packed bed reactor (left), from which the 2D axisymmetric representations (right; as used in the model) with 3, 5 and 9 beads are derived.

In the results part of the paper, we will use a few terms to refer to a specific part of the geometry. The "voids" refer to the open regions in the gas gap in between the packing beads. These open regions are connected to each other through so-called "void channels". The place in this void channel where the packing beads are closest to each other will be referred to as "contact point". Although the packing beads are not touching each other in this axisymmetric representation, in the real 3D geometry there would be the possibility for a contact point, as well as a void channel. In our previous paper [21] we accounted for both characteristics by applying 2 complementary 2D axisymmetric geometries, described by a so-called "contact-point" model and a "channel-of-voids" model, and we illustrated that the latter model, although there were no real contact points, was still able to predict the electric field enhancement near the contact points, like in the first model, but in addition was able to describe the movement of the discharge in between the beads, which is prohibited in the first model. Therefore, in this paper we include the void channels

instead of the direct contact points, since we do not want to isolate the voids from each other, removing their interconnected nature.

3. Results and discussion

3.1. Electric field enhancement

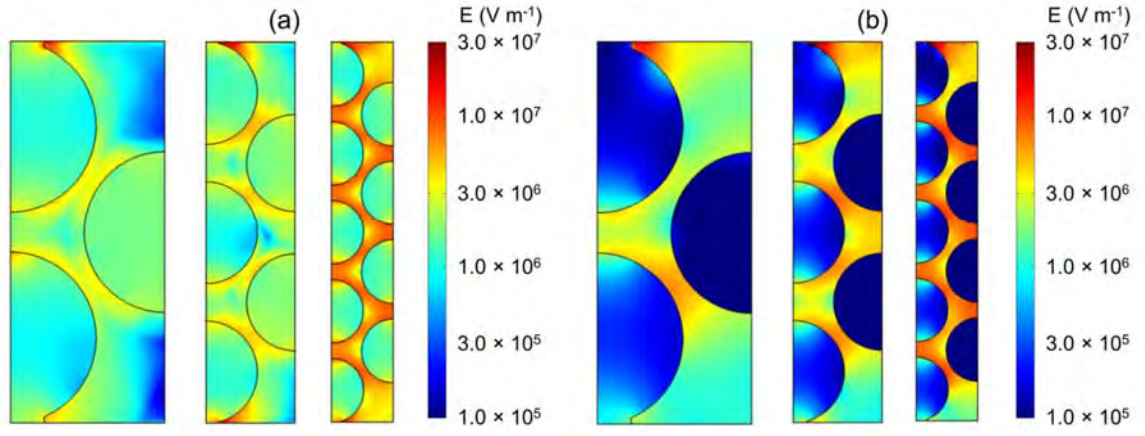

Figure 2: Time-averaged electric field strength for the geometry with 3, 5 and 9 beads, with a (a) zirconia packing (ε = 25) and (b) $BaTiO_3$ packing (ε = 1000).

In figure 2, we plot the time-averaged electric field strength over one cycle of applied potential (7.5 kV peak-to-peak) for the geometry with 3, 5 and 9 beads, with a zirconia packing (a) and a $BaTiO_3$ packing (b). It is clear that the electric field is enhanced near the contact points between the beads and the top dielectric or bottom electrode, and also in between the beads. As the packing beads get smaller, the enhancement clearly increases.

When comparing figure 2(a) and 2(b), we can see that, for a DBD reactor with single dielectric layer, at higher dielectric constant of the beads, the electric field enhancement shifts towards the dielectric layer covering the powered electrode, away from the uncovered grounded electrode. The same behaviour was observed in our previous study. [22] Furthermore, the overall

enhancement is also larger for packing beads with a higher dielectric constant. The 2D electron temperature profiles follow the same trend, and are therefore not specifically depicted in this paper. Their space- and time-averaged values will be discussed in section 3.3.

3.2. Electron density profiles

We are most interested in the behaviour of the plasma in the PBPRs, i.e., whether it can spread throughout the gap or stays localized between two beads. This information can be deduced from the time-averaged electron density plots, depicted in figure 3.

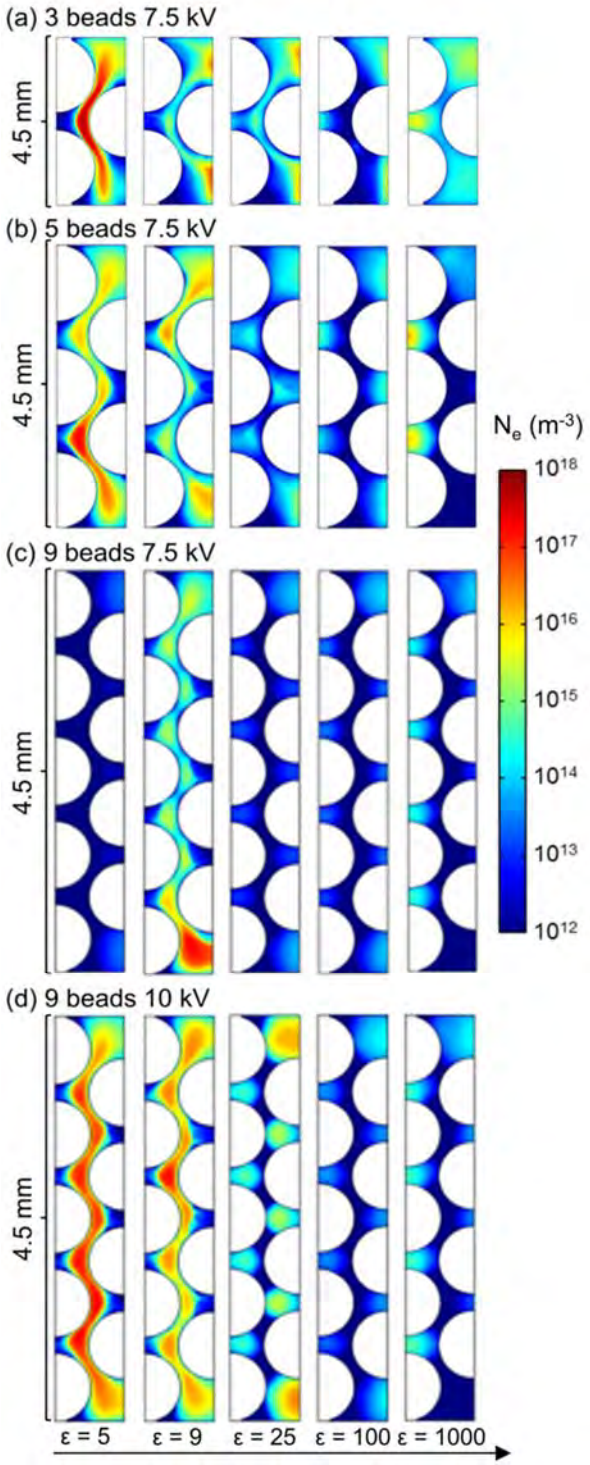

Figure 3: Time-averaged electron density profiles for the geometry with 3, 5 and 9 beads, with different dielectric constants. The result with 9 beads is also shown with a higher applied

potential of 10 kV peak-to-peak. Note that the different geometries have the same actual gap size, but were enlarged inversely to the decrease in bead size, for the sake of visibility.

Looking at the profiles of the 3 beads models (top row) as a function of increasing dielectric constant (from left to right), it is clear that for $\varepsilon = 5$ the electron density is maximum in the gaps between the beads, as if they only distort the plasma profile but do not influence the discharge behaviour. For $\varepsilon = 9$ and 25, the plasma can still pass through the gaps between the beads (the so-called "void channels"), but it shows a higher time-averaged electron density in the voids themselves. For $\varepsilon = 100$ and 1000 the plasma does not show significant electron density in the void channels, indicating that the plasma cannot pass through them anymore. The electron density stays localised in the voids, with lower values.

For the 5 beads models, the plasma can spread over the full gas gap up to $\varepsilon = 25$, although the maximum electron density clearly drops from 1.8×10^{17} at $\varepsilon = 5$ to 1.0×10^{14} m^{-3} at $\varepsilon = 25$. At $\varepsilon = 100$ and 1000, the electron density profiles show a clear density minimum in the region of the contact points, so the plasma is formed locally in the voids without an exchange of charged species between them, just as in the 3 beads models.

The 9 beads model packed with glass beads ($\varepsilon = 5$) and operated with an applied potential of 7.5 kV peak-to-peak, shows a very low overall electron density. As its electrical current profile will demonstrate below, no discharge is ignited in this setup. When the dielectric constant of the packing material is slightly higher, i.e. $\varepsilon = 9$, a discharge can be formed with significant electron density in the voids as well as in the void channels. At higher dielectric constants, the electron density drops significantly, and the plasma is limited to the voids. In other words, at $\varepsilon =$

25 and higher, the 9 beads model only shows localised, and quite weak, plasma formation at 7.5 kV peak-to-peak.

Because the 9 beads model did not ignite in the case of $\varepsilon = 5$ at the applied potential of 7.5 kV peak-to-peak and a frequency of 23.5 kHz, we also performed calculations at a higher applied potential of 10 kV peak-to-peak. At this higher applied potential, the plasma can clearly be ignited at the lowest dielectric constant, proven by the high electron density ($\sim 10^{17}$ m^{-3}). The discharge takes place again in the full gap, in line with the previous results for the 3 and 5 beads models and the lower dielectric constants. When the dielectric constant of the beads is increased to $\varepsilon = 9$, there is still significant electron density in the void channels, which is the indication of a full gap discharge. Further increasing the dielectric constant limits the electron density to the voids, indicating that from $\varepsilon = 25$ on, the discharge will again be localised.

3.3. Electric current profiles

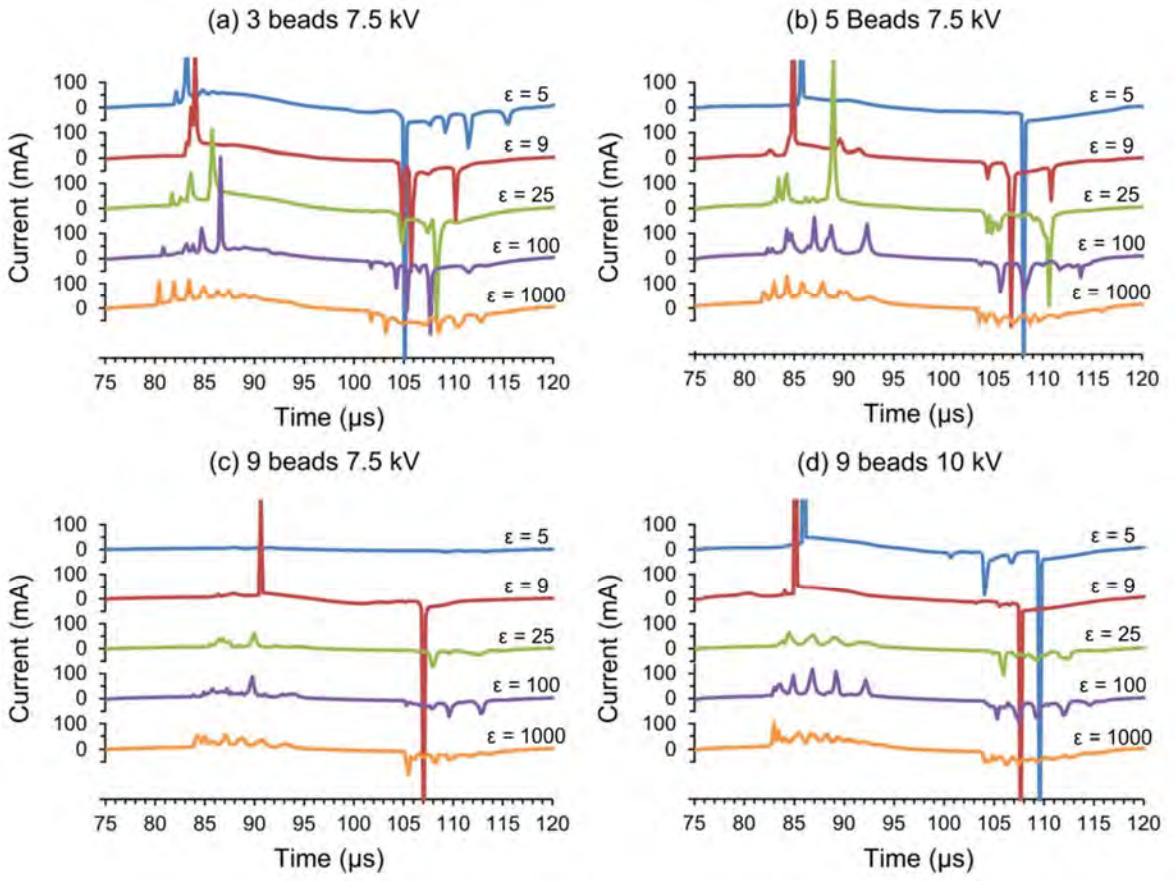

Figure 4: Current profiles calculated for the geometry with (a) 3 beads, (b) 5 beads and (c) 9 beads at 7.5 kV peak-to-peak applied potential, as well as (d) 9 beads with 10 kV peak-to-peak, for the different dielectric constants.

We can correlate the time-averaged electron density profiles with the calculated electric current profiles over a full cycle of the applied potential, as illustrated in figure 4. To calculate the current, the electrode surface area is needed. In the model this is the size of the circle formed by rotating the grounded electrode around the symmetry axis. However, to make the modelling results representative for a full size reactor, the current values are multiplied with a factor that comprises the ratio between the real electrode surface and the surface of the modelled disk. The value for the real electrode surface area is adopted from the cylindrical DBD reactor used in our

previous experimental study.[10] Because it is a cylindrical reactor, the average between the inner and outer surface area is taken.

It is clear from figure 4 that the current profile can change significantly as a function of dielectric constant, as well as bead size. Furthermore, within one current profile, the positive and negative half cycle can be fairly different as well. This difference is attributed to the fact that the PBPRs under study only have a single dielectric layer, which inherently makes the reactors asymmetrical. The significant change with packing size and dielectric constant, however, is obviously due to a change in discharge behaviour.

From the current profiles, two different types of current peaks can be distinguished, attributed to two types of discharges. The very strong current peaks, with intensity of several 100s to 1000 mA, originate from a discharge that can flow through the void channel covering the full gas gap. The smaller current peaks of a few 10s to 200 mA (and 400 mA in one exceptional occasion) are caused by a series of local discharges, which do not have the ability to cover the full gas gap. Around a few 100 mA, there is an overlap between the two possible discharges, which makes it difficult to unambiguously attribute the current peak to one of both possibilities, without looking at the instantaneous density profiles. This is due to the sampling frequency of the calculation results. During the course of the calculation, the results are written away at a frequency of 1/200 of one cycle of the applied potential. In some cases this frequency is not enough to resolve the full height of the current peak, resulting in lower values of a few 100 mA, where higher values are expected. The calculation time of a single model is in the order of a few weeks. Increasing the sampling frequency will drastically increase the calculation time even further, making it impractical. Therefore we opted to use the above mentioned frequency as a

best of both worlds: enough sampling points with a reasonable calculation time. We will now discuss the different current profiles in detail.

For the 3 beads models, strong current peaks are found at all dielectric constants except ε = 1000. At ε = 5, 9 and 25, the strongest current peak is attributed to a full gap discharge, while the other smaller current peaks are caused by local discharges. The order in which they occur can vary. Indeed, at ε = 25, the last current peak is caused by the full gap discharge, as also illustrated in our previous paper.[21] At lower dielectric constants, the full gap discharge can occur earlier, with the possibility of a few local discharges afterwards.

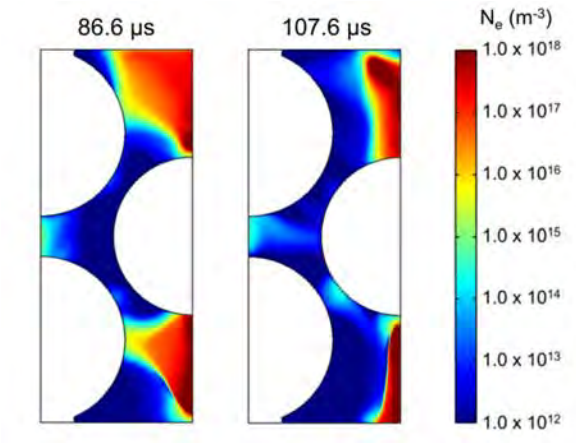

Figure 5: Instantaneous electron density profiles of the 3 beads model with ε = 100 packing beads for the largest current peak in the positive (86.6 µs) and negative (107.6 µs) half of the current profile.

The large current peaks at ε = 100 could be expected to also arise from a full gap discharge, but they are not. Looking at the instantaneous electron density profiles at the exact moment of the current peaks, shown in figure 5, we can conclude that they are the result of a local discharge taking place above and below the right packing bead in the geometry. This

illustrates that the current profiles alone cannot unambiguously give information of a certain discharge behaviour, but the latter can only be done when also studying the plasma density profiles. Hence, this clearly demonstrates the added value of modelling, to obtain detailed insight in the underlying mechanisms. Since the sizes of the void spaces in the 3 beads model are large compared to the models with more packing beads, the generated electrons by the aforementioned discharge can accumulate to higher numbers before hitting a wall, giving rise to a stronger current peak.

At even higher dielectric constant (ε =1000), no discharge can take place anymore at the same time above and below the right packing bead. The electric field enhancement shifts away from the grounded electrode, as mentioned before, restricting the plasma generation to the top part of the reactor, resulting in a larger number of short-lived local discharges, and thus a larger number of smaller current peaks. This observation was also found experimentally by Ohsawa et al., who investigated the discharge characteristics in a parallel plate reactor packed with a disc of fused glass beads.[34] In their study the current profile of the discharge with the smallest packing beads (0.105 – 0.212 mm) showed much more, and smaller, current peaks (~ 0.2 mA) than the current profile with the largest beads (3 mm), which consisted of less but stronger current peaks (~ 10 mA).

The 5 beads model clearly follows the same trend. At ε = 5, 9 and 25, one strong current peak is found per half cycle, attributed to a full gap discharge, and with an increasing number of smaller current peaks upon rising dielectric constant. At ε = 100, no full gap discharge is taking place anymore, and all the smaller current peaks (< 200 mA) arise from local discharges. At ε = 1000, we observe the largest number of current peaks, but they are also the smallest (< 100 mA), again originating from localised discharges.

For the 9 beads model at 7.5 kV peak-to-peak and ε = 5, no discharge can be ignited (see above), explaining the absence of current peaks. Obviously the applied potential is not high enough to cause a breakdown anywhere in the reactor. Indeed, because the dielectric constant of the packing material (ε = 5) is rather low, the electric field enhancement in the reactor between the beads will also be small. However, already at slightly higher dielectric constant, the electric field enhancement will be larger, which explains why at ε = 9 a discharge can be formed. It is a full gap discharge, with one large current peak each half cycle. At ε = 25, no full gap discharge can be formed anymore, illustrated by the larger number of smaller current peaks, caused by local discharges. The smaller bead size in combination with the higher dielectric constant enhances the electric field near the contact points, so that the electrons are accelerated more towards the bead walls, and not being able to pass through the void channel anymore. Increasing the dielectric constant further does not change the plasma characteristics very much, as is obvious from the current profiles in figure 4.

When the applied potential is increased to 10 kV peak-to-peak, the plasma can clearly be ignited at the lowest dielectric constant, enforcing the statement that the size of the packing beads as well as their dielectric constant both have an influence on the breakdown voltage (see below). The discharge takes place again over the full gap, as expected for this low dielectric constants. At ε = 9 it is still a full gap discharge, but in contrast to the results at the lower applied potential, a few minor current peaks pop up before the large current peak. At ε = 25 and higher, the intensity of the current peaks drops, while the number of peaks rises, indicative for the current profile of localised plasma formation.

The fact that a lower dielectric constant requires a higher breakdown voltage corresponds well with experiments performed by Butterworth et al., who reported that the use of $BaTiO_3$ (ε =

1000 and higher) as packing material could lead to plasma formation at an applied potential of 10 kV peak-to-peak, while the minimum required potential for alumina packing ($\varepsilon = 9$) was 16 kV peak-to-peak.[23] Furthermore, the observation that a smaller bead size requires a higher breakdown voltage is also shown experimentally by Butterworth et al.[23] For both a packing of $BaTiO_3$ or Al_2O_3, the authors reported that a decreasing bead size resulted in an increasing breakdown voltage.

3.4. Summarizing results

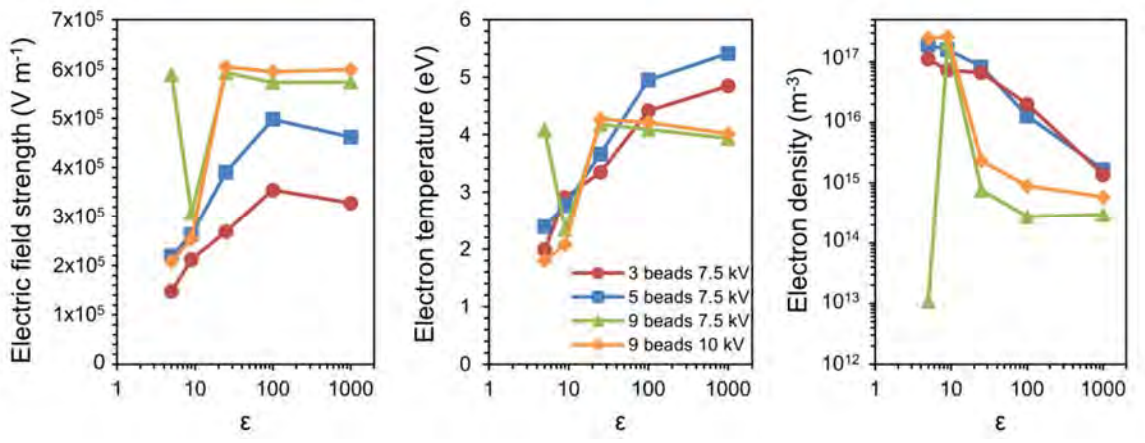

Figure 6: Influence of the dielectric constant on the space- and time-averaged electric field strength, electron temperature and electron density, for the geometry with 3 beads, 5 beads and 9 beads (both at 7.5 and 10 kV peak-to-peak).

Figure 6 summarizes the influence of the dielectric constant on the three key plasma parameters, namely the electric field strength, electron temperature and electron density. The values are averaged in time over one cycle of the applied potential, and in space, over the entire reactor geometry.

As illustrated in figure 2 above, the electric field strength increases with increasing dielectric constant of the packing beads. Indeed, a higher dielectric constant will lead to stronger polarization of the dielectric material and therefore a greater difference between close-by opposite charges in the vicinity of the contact points between the dielectric objects. The enhancement of the electric field strength was experimentally proven by Mei et al., showing a clear increase when switching from a glass to a $BaTiO_3$ packing of similar size.[9]

However, at a certain dielectric constant, the enhancement stagnates, as appears from figure 6. In literature, this phenomenon was first reported by Chen et al., based on calculations with the spherical void model of Takaki et al.[15, 26] In their study the electric field enhancement stagnated around a dielectric constant of 100. Our 3 beads and 5 beads model follow the same trend, with a maximum electric field enhancement at $\varepsilon = 100$. When the packing beads are smaller (i.e. in the 9 beads model), the saturation in electric field enhancement happens already at $\varepsilon = 25$.

Furthermore, a smaller packing also implies a higher overall electric field strength. The maximum electric field strength is indeed almost a factor 2 higher for the 9 beads model (0.75 mm diameter) compared to the 3 beads model (2.00 mm diameter). Note that the results for the 9 beads model operated at 7.5 kV peak-to-peak with a glass packing ($\varepsilon = 5$) show an exceptionally high electric field (and a very low electron density; see below), since this set-up does not exhibit plasma formation, as mentioned before. The applied potential is indeed too low to cause a discharge, and therefore the electric field is always high, because it is never distorted or lowered by the presence of plasma.

The electron temperature roughly follows the same trend as the electric field strength, with an increase in overall value upon rising dielectric constant. The saturation observed for the

electric field in the geometry with 3 and 5 beads is also partially reflected in the electron temperature, although the value still rises above $\varepsilon = 100$. For the 9 beads model, the stagnation appears at exactly the same dielectric constant, namely $\varepsilon = 25$. On the other hand, the effect of bead size is clearly different for the electron temperature and the electric field strength. Decreasing the bead diameter from 2.00 mm (3 beads) to 1.20 mm (5 beads) increases the electron temperature, especially at higher dielectric constants, just like for the electric field strength. Smaller packing beads with diameter of 0.75 mm, however, do not lead to a further increase in overall electron temperature as they do with the electric field strength. This is probably related to the low electron density in the 9 beads model for $\varepsilon = 25$ or above (see below).

The time- and space-averaged electron density clearly drops upon rising dielectric constant of the packing, as could also be deduced from figure 3 above. For the 3 and 5 beads model, the electron density decreases only slightly between $\varepsilon = 5$ and 25, but afterwards it drops by several orders of magnitude. For the 9 beads models, the electron density drops two orders of magnitude above $\varepsilon = 9$, but afterwards it only slightly decreases between $\varepsilon = 25$ and 1000. This drop can be explained as follows. As the electric field strength increases, the electrons can move faster, which will increase their loss rate at the walls, resulting in a lower overall electron density. Reducing the size of the packing beads has the same effect on this loss rate. Indeed, the walls are closer to each other, so the electrons will hit the walls faster, again leading to lower electron densities.

This can be illustrated by looking at figure 7, which shows the collision rate (a) and (a measure of) the collision frequency (b) of the electrons at the surface of the beads, integrated over all beads in the reactor. The collision rates are all relatively close to each other, except for the 9 beads model at $\varepsilon = 5$, because no discharge could be formed there. However, the number of

electrons hitting the different surfaces is of course directly related to the electron density in the reactor. Indeed, if the electron density is low, the collision rate will be low, as indicated by the first point of the 9 beads model where no plasma was present. Therefore, dividing the collision rate by the average electron density in the reactor yields a good measure of the relative ease at which the electrons get lost at the walls, and this is plotted in figure 7(b), showing a clear increasing trend from low to high dielectric constants, and from large to smaller beads (at least for ε above 10).

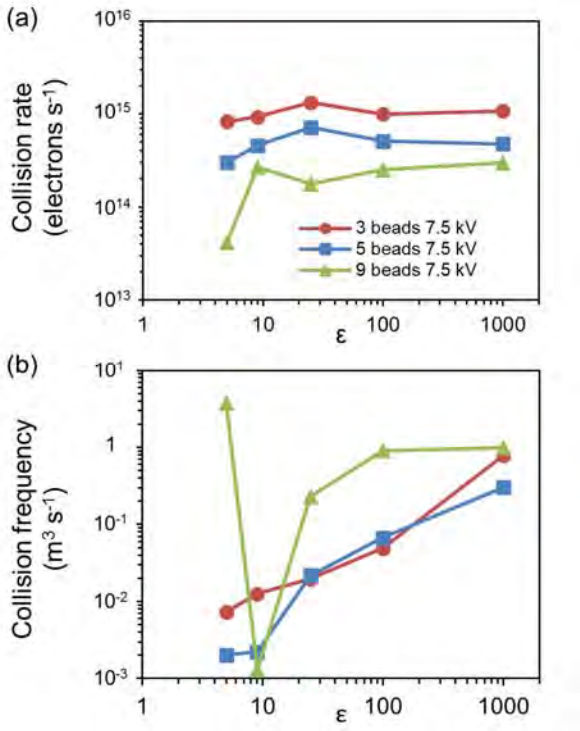

Figure 7: Influence of the dielectric constant and bead size on the time-averaged collision rate (a) and (a measure of) the collision frequency (b) of the electrons at the walls of the beads, integrated over the surface of all beads in the reactor.

When comparing the results for the different bead sizes, we can conclude that at low dielectric constants, the electric field strength, electron temperature and density in case of 3 beads, 5 beads and 9 beads are all close to each other. This can be explained by the type of discharge taking place. As shown in figure 3 above, at low dielectric constant, the plasma does not exist locally, but can flow through the void channels over the full gap of the reactor. This so-called full gap discharge takes place regardless of the size of the packing beads, as long as the dielectric constant is low enough (i.e. up to 25, depending on the bead size), and it is not heavily affected by the presence of the packing beads.. On the other hand, at higher dielectric constants, the discharges become localised, and they are fully defined by the packing, so the plasma parameters will be very different for different bead sizes.

To summarise, when the dielectric constant increases, the electric field is more enhanced, leading to more energetic electrons, i.e. a higher electron temperature, resulting in more electron dissipation at the walls, and thus a lower electron density. Decreasing the size of the packing beads leads to a higher electric field strength, but as a consequence, also to a lower electron density.

These model predictions are very useful for a better insight in the experimental work with PBPRs to help clarify the experimentally observed trends in e.g. CO_2 conversion and energy efficiency as a function of bead size and dielectric constant. However, the reader must be aware that the values of applied potential, together with the resulting current profile, electric field strength, electron temperature and electron density all apply to a helium plasma, and cannot directly be transferred to other discharge gases. CO_2 for example, requires a significantly higher voltage to reach breakdown than helium, as can be deduced from the shape and location of their respective Paschen curves.[35] Therefore, our results are not quantitatively transferable from

helium to CO_2, but only qualitatively. Indeed, the observed trends can be expected to stand, albeit at different values of applied potential and with a different plasma behaviour (i.e., uniform plasma for helium, vs. combination of streamers and surface discharges for a molecular gas). Furthermore, it needs to be stressed that all other material properties besides the dielectric constant, which are inherently present in experiments, are not taken into account yet in our model. Nevertheless, in the following section we attempt to correlate our modelling results, which focus only on the influence of the dielectric constant, to experimentally observed trends for CO_2 conversion, still keeping the above considerations in mind.

It is important to remember that, in terms of the possible influence of dielectric constant, the combination of both an enhanced electric field with a sufficient electron density would be necessary to improve the experimental performance. This is quite challenging because a higher electric field strength is usually accompanied by a lower electron density (figure 6).

Michielsen et al. found the best CO_2 conversions and efficiencies with a $BaTiO_3$ packing with the largest bead size.[24] $BaTiO_3$ has the highest dielectric constant and thus the most enhanced electric field compared to the other tested materials, although the electron density is lower. On the other hand, the best performing bead size was the largest, meaning that the electric field strength will not be enhanced even further, but in return, the electron density will remain relatively high. In other words, large beads with a high dielectric constant seem to give the best combination between enhancement of the electric field strength and reasonable electron density, in good agreement with our model predictions (see figure 6).

The exact same explanation can be given for the results of Butterworth et al. with 100 % CO_2, where $BaTiO_3$ provided the best results when the bead size was the largest.[23]

In our previous study, the highest CO_2 conversions were also found with the largest packing beads, provided that the input power is not too high (60 W).[10] However, at the highest input power (100 W), the smaller beads perform better. This can also be explained based on our modelling results. One would expect that at higher input power, the largest beads perform better, because the electron density will still be high enough, as the loss rates at the bead surfaces are expected to decrease upon larger beads. However, in this case, the breakdown voltage plays a role, because in the reactor packed with smaller beads at lower input power, the breakdown voltage is less often met (see figure 3), resulting in a lower discharge rate and conversion compared to a reactor with larger beads (and thus a lower breakdown voltage). At higher input power, the breakdown voltage is more often met in the smaller beads reactor, resulting in a significantly higher conversion, while the change for the larger beads can be less significant.

Finally, Duan et al. reported that the highest dielectric constant (only $\varepsilon \sim 12$) resulted in the best performance, as expected. However, in their study, the smallest beads (0.18 – 0.25 mm) performed better. The explanation is two-fold. First of all, when the diameter of the largest beads (0.25 – 0.42 mm) is around half the size of the gas gap (0.6 mm), a lot of open space exists in the discharge gap, due to imperfect stacking of the beads. The number of contact points, where the electric field strength will be enhanced, is thus much lower, lowering the overall electric field enhancement significantly, and therefore resulting in lower CO_2 conversions. In this case, the ideal size of the packing beads is therefore not simply the largest one, but the largest without disturbing the ability to form a close packed system. Secondly, we need to realize that the dielectric constant is not necessarily the only factor driving the maximum conversion. Indeed, as stated in the introduction, CaO has the ability to capture CO_2 and this will affect the measured

conversion. Smaller beads correspond to a larger surface area at which CO_2 can be captured, thereby also increasing the amount of CO_2 lost in the reactor.

As mentioned before, we stress again that next to the dielectric constant, a whole range of material properties can influence the conversion rate, as demonstrated by the examples in the introduction.[8, 24] However, in our modelling study we only focus on one property, which enables us to explain already a great deal of the experimental results on environmental applications based on this property alone. We therefore believe that the dielectric constant is an important material property to consider when trying to reach a higher conversion rate in the applications.

Conclusion

We studied the effect of bead size and dielectric constant on the plasma behavior in a packed bed DBD reactor by means of a fluid model. Our calculations illustrate that the plasma behavior can change significantly when changing these parameters. At low dielectric constant of the packing beads, the plasma is always a so-called “full gap” discharge, irrespective of the bead size, i.e., the plasma is spread out over the full gas gap, showing significant density in the voids as well as in the connecting void channels. The electric current profile shows one (or two) strong current peaks per half cycle, attributed to the full gap discharge, the electron density is relatively high, while the electric field strength and electron temperature are rather low.

When the dielectric constant increases, the electric field enhancement at the contact points (or the position of smallest void channel) is so high that the electrons are accelerated to the walls of the beads, rather than having the ability to flow through the void channel. The plasma can no

longer extend from one void to a neighboring void and it becomes localised. The current profile will change from one large peak per half cycle to a lot of smaller peaks, each arising from an individual local discharge somewhere in the reactor. The time-averaged electric field strength is higher, as mentioned above, leading to a higher electron temperature, but a lower electron density, because the electrons get lost more easily at the walls. At larger bead sizes, the shift from full gap discharge to localised discharges will occur at a higher dielectric constant, which is logical, because of the larger voids in between the larger beads. Finally, smaller bead sizes or a lower dielectric constant of the beads will require a higher breakdown voltage, which corresponds well with experimental results. These model predictions help to clarify the experimentally observed trends, providing us with a better insight in the experimental work with PBPRs.

Acknowledgements

K. Van Laer is indebted to the Institute for the Promotion of Innovation by Science and Technology in Flanders (IWT Flanders) for financial support. This research was carried out in the framework of the network on Physical Chemistry of Plasma-Surface Interactions - Interuniversity Attraction Poles, phase VII (http://psi-iap7.ulb.ac.be/), and supported by the Belgian Science Policy Office (BELSPO). The calculations were carried out using the Turing HPC infrastructure at the CalcUA core facility of the Universiteit Antwerpen (UAntwerpen), a division of the Flemish Supercomputer Center VSC, funded by the Hercules Foundation, the Flemish Government (department EWI) and the UAntwerpen.

References

[1] K. Schmidt-Szalowski and A. Borucka, Plasma Chem. Plasma Proc., 9, 235 (1989)

[2] S. Jodzis, Ozone-Sci. Eng., 25, 63 (2003)

[3] H. L. Chen, H. M. Lee and M. B. Chang, Ozone: Sci. Eng., 28, 111 (2006)

[4] C.L. Chang and T.S. Lin, Plasma Chem. Plasma Proc., 25, 227 (2005)

[5] H.X. Ding, A.M. Zhu, X.F. Yang, C.H. Li and Y. Xu, J. Phys. D: Appl. Phys., 38, 4160 (2005)

[6] M. Kraus, B. Eliasson, U. Kogelschatz and A. Wonkaun, Phys. Chem. Chem. Phys., 3, 294 (2001)

[7] H.L. Chen, H.M. Lee, S.H. Chen, Y. Chao and M.B. Chang, Appl. Catal. B: Environ., 85, 1 (2008)

[8] Q. Yu, M. Kong, T. Liu, J. Fei and X. Zheng, Plasma Chem. Plasma Process., 32, 153-163 (2012)

[9] D. Mei, X. Zhu, Y. He, J.D. Yan and X. Tu, Plasma Sources Sci. Technol., 24, 015011 (2015)

[10] K. Van Laer and A. Bogaerts, Energy Technol., 3, 1038-1044 (2015)

[11] A. Gómez-Ramírez, A.M. Montoro-Damas, M.A. Rodríguez, A.R. González-Elipe and J. Cotrino, Chem. Eng. J., 314, 311-319 (2017)

[12] E.C. Neyts and A. Bogaerts, J. Phys. D: Appl. Phys., 47, 224010 (2014)

[13] E.C. Neyts, K. Ostrikov, M.K. Sunkara and A. Bogaerts, Chem. Rev., 115, 13408-13446 (2015)

[14] J.S. Chang, K.G. Kostov, K. Urashima, T. Yamamoto, Y. Okayasu, T. Kato, T. Iwaizumi and K. Yoshimura, IEEE Trans. Ind. Appl., 36, 1251 (2000)

[15] K. Takaki, J.S. Chang and K.G. Kostov, IEEE Trans. Dielectr. Electr. Insul., 11, 481 (2004)

[16] W.S. Kang, J.M. Park, Y. Kim and S.H. Hong, IEEE Trans. Plasma Sci., 31, 504 (2003)

[17] H. Russ, M. Neiger and J.E. Lang, IEEE Trans. Plasma Sci., 27, 38 (1999)

[18] N.Y. Babaeva and M.J. Kushner, Plasma Sources Sci. Technol., 18, 035009 (2009)

[19] J. Kruszelnicki, K.W. Engeling, J.E. Foster, Z. Xiong and M.J. Kushner, J. Phys. D: Appl. Phys., 50, 025203 (2017)

[20] Y. Zhang, H. Wang, W. Jiang and A. Bogaerts, New J. Phys., 17, 083056 (2015)

[21] K. Van Laer and A. Bogaerts, Plasma Sources Sci. Technol., 25, 015002 (2016)

[22] K. Van Laer and A. Bogaerts, Plasma Process. Polym., published online (2016) DOI: 10.1002/ppap.201600129

[23] T. Butterworth, R. Elder and R. Allen, Chem. Eng. J., 293, 55-67 (2016)

[24] I. Michielsen, Y. Uytdenhouwen, J. Pype, B. Michielsen, V. Meynen and A. Bogaerts, DOI: 10.1016/j.cej.2017.05.177

[25] X. Duan, Z. Hu, Y. Li and B. Wang, AIChE J., 61, 898 (2015)

[26] H.L. Chen, H.M. Lee, S.H. Chen and M.B. Chang, Ind. Eng. Chem. Res., 47, 2122-2130 (2008)

[27] S.K.P. Veerapandian, C. Leys, N. De Geyter and R. Morent, Catalysts, 7, 113 (2017)

[28] X. Lu, G.V. Naidis, M. Laroussi, S. Reuter, D.B. Graves and K. Ostrikov, Phys. Rep., 630, 1-84 (2016)

[29] X. Lu, G.V. Naidis, M. Laroussi and K. Ostrikov, Phys. Rep. 540, 123-166 (2014)

[30] N. Y. Babaeva, A.N. Bhoj and M.J. Kushner, Plasma Sources Sci. Technol. 16, 591-602 (2006)

[31] N.Y. Babaeva and M.J. Kushner, Plasma Sources Sci. Technol., 20, 035018 (2011)

[32] http://www.comsol.com

[33] D. Petrovic, T. Martens, J. van Dijk, W.J.M. Brok and A. Bogaerts, J. Phys.: Conf. Ser., 133, 012023 (2008)

[34] A. Ohsawa, R. Morrow and A. B. Murphy, J. Phys. D: Appl. Phys., 33, 1487-1492 (2000)

[35] E. Hastings, G. Weyl and D. Kaufman, J. Spacecraft Rockets, 27, 539 (1990)